14th Australasian Fluid Mechanics Conference
Adelaide University, Adelaide, Australia
10-14 December 2001

Performance of an Energy - Temperature Dissipation Rate Probe in Decaying Grid Turbulence

T. Zhou[1], R. A. Antonia[2] and L. P. Chua[1]

**[1] School of Mechanical and Production Engineering
Nanyang Technological University, Singapore 639798
[2] Department of Mechanical Engineering,
The University of Newcastle, NSW 2308, AUSTRALIA**

Abstract

Instantaneous energy and temperature dissipation rates are measured simultaneously in decaying grid turbulence using a probe consisting of 4 X-wires (a total of 8 hot wires operated in constant temperature mode) and 2 pairs of parallel cold wires (operated in constant current mode). The directly measured mean values of the energy and temperature dissipation rates agree, within ±10%, with those obtained from the decay rates of the mean turbulent energy and temperature variance. The probe also yields all three fluctuating vorticity components; after correction for spatial resolution, their spectra are in close agreement with isotropic calculations over nearly all wavenumbers. The vorticity variance decays with the same power-law behaviour as the mean energy dissipation rate. Transport equations for the mean energy and temperature dissipation rates are satisfied, within ±10%, by the data obtained from this probe.

Introduction

Measurements of the energy dissipation rate $\varepsilon \equiv 2\nu s_{ij}s_{ij}$ and the temperature variance dissipation rate $\chi \equiv \kappa\theta_{,i}\theta_i$ separately in turbulent flows have been conducted by quite a number of researchers (e.g. [1,2]), where $s_{ij} \equiv (u_{i,j}+u_{j,i})/2$ is the turbulent rate of strain, $u_{i,j}$ represents the velocity derivative $\partial u_i/\partial x_j$ and ν is the kinematic viscosity of the fluid; $\theta_{,i}$ represents the temperature derivative $\partial\theta/\partial x_i$ and κ is the thermal diffusivity of the fluid. Although these two quantities are available simultaneously in direct numerical simulation databases, simultaneous measurements of ε and χ have, to our knowledge, never been attempted. Such measurements are important when the correlation between ε and χ is required. They are also important for examining the extension to passive scalars of Kolmogorov's refined similarity hypothesis (RSHP) (e.g. [3]). The correlation between suitable powers of ε and χ appears in RSHP. However, measurements of ε and χ are not straightforward since multiple cold wire probes need to be operated simultaneously with multiple hot wire probes. As the number of wires increases, problems related to spatial resolution, noise contamination and possibly aerodynamic interference become important (e.g. [4,5]). The simplest way to estimate ε and χ is by assuming isotropy, viz.

$$\varepsilon_{iso} = 15\nu(\partial u_1/\partial x_1)^2 \qquad (1)$$

$$\chi_{iso} = 3\kappa(\partial\theta/\partial x_1)^2 \qquad (2)$$

where u_1 is the velocity fluctuation in the streamwise (x_1) direction and θ is the temperature fluctuation. It is also generally assumed that $\partial u_1/\partial x_1$ and $\partial\theta/\partial x_1$ can be estimated from $\partial u_1/\partial t$ and $\partial\theta/\partial t$ by using Taylor's hypothesis. The present study represents the first attempt to measure these two quantities simultaneously in a decaying grid turbulence. In this flow, the true values of $\langle\varepsilon\rangle$ and $\langle\chi\rangle$ are known with relatively high accuracy from the rates of decay of the mean energy $\langle q^2\rangle (\equiv \langle u_1^2\rangle + \langle u_2^2\rangle + \langle u_3^2\rangle)$ (angular brackets denote time averaging) and the temperature variance $\langle\theta^2\rangle$, viz.

$$\langle\varepsilon\rangle_d = -\frac{U_1}{2}\frac{\partial\langle q^2\rangle}{\partial x_1} \qquad (3)$$

$$\langle\chi\rangle_d = -\frac{U_1}{2}\frac{\partial\langle\theta^2\rangle}{\partial x_1} \qquad (4)$$

where the subscript d denotes values obtained from the rates of decay so that the performance of the probe in measuring $\langle\varepsilon\rangle$ and $\langle\chi\rangle$ can be "calibrated". This is an important prerequisite if the instantaneous values of ε and χ, obtained with this probe, are to be trusted.

Experimental Details

The experiment was conducted in a wind tunnel with a Taylor microscale Reynolds number R_λ of about 40 [$R_\lambda \equiv u_1'\lambda/\nu$, the prime denotes the rms value and $\lambda \equiv u_1'/(\partial u_1/\partial x_1)'$ is the longitudinal Taylor microscale]. The probe consisting of four X-wires and two pairs of parallel cold-wires is shown in Figure 1. The separation between two inclined wires in each X-probe is about 0.8mm. The separations between centers of X-probes are $\Delta x_2 \equiv 2.0$mm and $\Delta x_3 \equiv 2.5$mm in the x_2 and x_3 directions, respectively. The effective angle for each inclined wire is about 40^o. The separations of the parallel cold-wires are $\Delta x_2 \equiv 2.0$mm and $\Delta x_3 \equiv 2.5$mm respectively. These four cold wires can measure all three temperature derivatives that appear in the full expression of χ. Details of flow conditions can be found in Zhou et al. [6].

The hot and cold wires were etched from Wollaston (Pt-10% Rh) wires. The active lengths are about $200d_w$ and $800d_w$ for the hot and cold wires respectively (where d_w is the wire diameter, equals to 2.5μm for the hot wires and 1.27μm for the cold wires). The hot wires were operated with in-house constant temperature circuits at an overheat ratio of 0.5. The cold wires were operated with constant current (0.1 mA) circuits. The probe was calibrated at the centerline of the tunnel against a Pitot-static tube connected to a MKS Baratron pressure transducer (least count = 0.01 mm H_2O). The yaw calibration was performed over $\pm 20^o$. Output signals from the anemometers were passed through buck and gain circuits and low-pass filtered at a cut-off frequency f_c ranging between 1250 Hz (at $x_1/M=20$) to 800 Hz (at $x_1/M=80$). The value of f_c was generally close to $U_1/2\pi\eta$, which is commonly identified as the Kolmogorov frequency f_K. The filtered signals

were subsequently sampled at a frequency f_s =2 f_c using a 12-bit A/D converter. The record duration was about 90s.

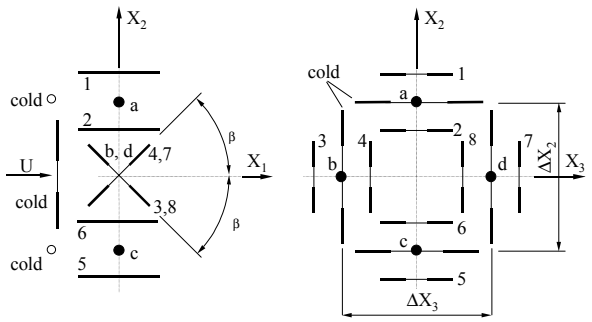

(a) Side view (b) Front view

Figure 1. Sketches of the probe.

Experimental Results

With the 4 X-wire probe, <ε> can be approximated by assuming continuity (e.g. [7]) ,

$$<\varepsilon>_{ful}=\nu\{4<u_{1,1}^2>+<u_{1,2}^2>+<u_{1,3}^2>+<u_{2,1}^2> +<u_{3,1}^2>+<u_{2,3}^2>+<u_{3,2}^2>+2<u_{1,2}u_{2,1}> +2<u_{1,3}u_{3,1}>-2<u_{2,3}u_{3,2}>\quad (5)$$

The three vorticity components were also obtained from the measured u_i, viz.

$$\omega_1=u_{3,2}-u_{2,3}\approx\frac{\Delta u_3}{\Delta x_2}-\frac{\Delta u_2}{\Delta x_3} \quad (6)$$

$$\omega_2=u_{1,3}-u_{3,1}\approx\frac{\Delta u_1}{\Delta x_3}-\frac{\Delta u_3}{\Delta x_1} \quad (7)$$

$$\omega_3=u_{2,1}-u_{1,2}\approx\frac{\Delta u_2}{\Delta x_1}-\frac{\Delta u_1}{\Delta x_2} \quad (8)$$

where $u_{i,j}\equiv\partial u_i/\partial x_j$. Δu_3 and Δu_1 in (6) and (8) respectively are velocity differences between X-probes a and c (Figure 1); Δu_2 and Δu_1 in (6) and (7) respectively are velocity differences between X-probes b and d. Derivatives in the x_1 direction were estimated using Taylor's hypothesis, i.e. $\partial/\partial x_1=-U_1\partial/\partial t$. Because of the low turbulence ($u_i'/U_1 \le 2\%$, where i = 1,2,3), the use of Taylor's hypothesis should be satisfactory.

With the four cold wires, the full temperature dissipation rate <χ> can then be obtained, viz.

$$<\chi>_{ful}=\kappa\{<\theta_{,1}^2>+<\theta_{,2}^2>+<\theta_{,3}^2>\}. \quad (9)$$

Again, Taylor's hypothesis was used to convert temporal derivatives to longitudinal spatial derivatives.

Since the correct selection of wire separation is crucial for derivative measurements, a preliminary experiment was conducted to determine the optimum separation of the wires. Details of these results can be found in [6]. The present probe configuration was based on those optimum values. Before presenting statistics for u_i or ω_i, it is relevant to address the effect of the imperfect spatial resolution of the probe on the measurements. The high wavenumber part of the velocity spectrum and, more especially, the vorticity spectrum is expected to be attenuated due to this imperfect resolution. Detailed expressions for this attenuation were given in [5] for the three-component vorticity probe. The corrected spectra of ω_i (i=1,2,3) at the measurement location x_1/M=40 are shown in Figure 2. Here the spectrum ϕ_α is defined such that $\int_0^\infty\phi_\alpha dk_1=<\alpha^2>$. Also shown for comparison are the spectra calculated using isotropic relations in terms of $\phi_{u_{1,1}}$ (e.g. [8]),

$$\phi_{\omega_1}(k_1)=\phi_{u_{1,1}}(k_1)+4\int_{k_1}^\infty\frac{\phi_{u_{1,1}}(k)}{k}dk \quad (10)$$

$$\phi_{\omega_2}(k_1)=\phi_{\omega_3}(k_1)=\frac{5}{2}\phi_{u_{1,1}}(k_1)-\frac{k_1}{2}\frac{\partial\phi_{u_{1,1}}(k_1)}{\partial k_1} +4\int_{k_1}^\infty\frac{\phi_{u_{1,1}}(k_1)}{k}dk \quad (11)$$

This comparison provides a performance check of the probe in measuring ω_i as well as a check for local isotropy. The agreement between corrected spectra and corresponding isotropic calculations is quite good at all wavenumbers even at such a small value of R_λ, reflecting the association of vorticity mainly with small scales.

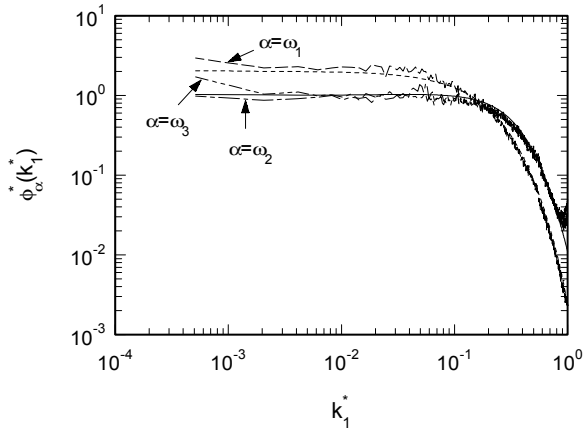

Figure 2. Comparison of measured vorticity spectra with isotropic calculations. Measured: — —: α=ω1; — - —, ω2; — - - —, ω3. Calculated: - - -, ω1 (Eq. 10); —, ω2 (or ω3) (Eq. 11).

The values of $<\varepsilon>_d$ and $<\chi>_d$ obtained via (3) and (4) provide benchmarks for <ε> and <χ>. From x_1 derivatives of $<q^2>$ and $<\theta^2>$, estimates of $<\varepsilon>_d$ and $<\chi>_d$, which decay with power-law exponents of 2.3 and 2.4 respectively, can be obtained. They are shown as dashed lines in Figures 3(a,b). Also shown in these figures are the measured values of $<\varepsilon>_{ful}$ and $<\chi>_{ful}$ obtained using Eqs. (5) and (9) and values of $<\varepsilon>_{iso}$ and $<\chi>_{iso}$. Because of the imperfect spatial resolution of the cold wire arrangement for $x_1/M \le 50$, the derivatives in Eq. (9) were also corrected. Details for temperature derivative corrections can be found in Antonia and Mi [9]. The favourable agreement (within ±10%) between either $<\varepsilon>_{ful}$ [Eq. (5)], $<\varepsilon>_d$ and $<\varepsilon>_{iso}$ (Figure 3a) or $<\chi>_{ful}$ [Eq. (9)], $<\chi>_d$ and $<\chi>_{iso}$ (Figure 3b) indicates that $<\varepsilon>_{ful}$ and $<\chi>_{ful}$ can be estimated adequately with the present probe.

Assuming local isotropy, the three vorticity components are related to the value of $< u_{1,1}^2 >$, viz.

$$< \omega_1^2 >=< \omega_2^2 >=< \omega_3^2 >= 5 < u_{1,1}^2 > \qquad (12)$$

Eq. (12) has been verified in [7]. We have also verified it in this study to an accuracy of ±10% (Figure 4).

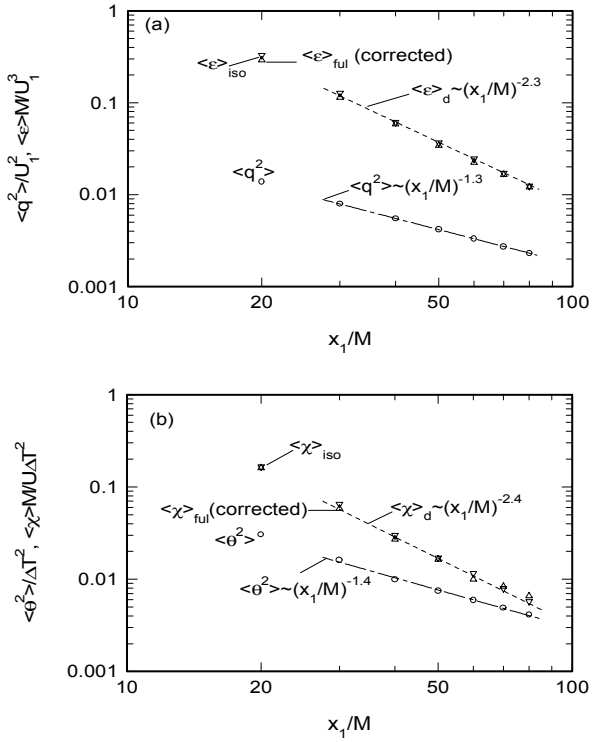

Figure 3. Streamwise decay of (a): $<q^2>$ and $<\varepsilon>$, (b): $<\theta^2>$ and $<\chi>$. ΔT is the mean temperature above ambient. o: $<q^2>$ and $<\theta^2>$; ∇: $<\varepsilon>_{iso}$ and $<\chi>_{iso}$; Δ: $<\varepsilon>_{ful}$ (Eq. 5) and $<\chi>_{ful}$ (Eq. 9). Lines are power-law fit.

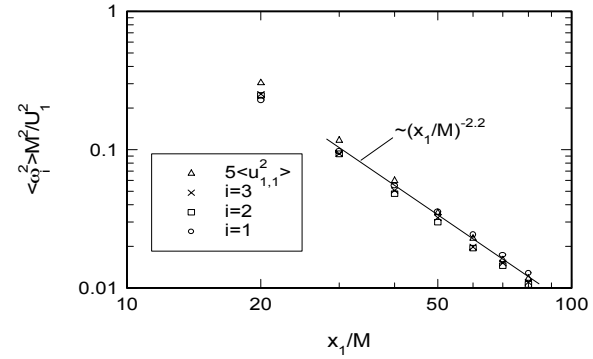

Figure 4. Components of mean square vorticity and comparison with isotropy. The solid line is the power-law fit to the measured vorticity variances.

The equation describing the rate of change of enstrophy $<\omega^2>$ ($\equiv<\omega_i\omega_i>$) or equivalently $<\varepsilon>/\nu$ in homogeneous isotropic turbulence was first derived by von Kármán [10]

$$\frac{d < \varepsilon >}{dt} = 2\nu < \omega_i \omega_j u_{i,j} > +2\nu^2 < \omega_i \nabla^2 \omega_i > \qquad (13)$$

The two invariants on the right side of (13) represent the creation of $<\varepsilon>$ through the stretching of vorticity by the turbulent strain rate field and the destruction of $<\varepsilon>$ through the action of viscosity. Using the isotropic forms of $<\omega_i\omega_j u_{i,j}>$ and $<\omega_i\nabla^2\omega_i>$, Eq. (13) can be simplified to the equation obtained by [11], viz.

$$-U_1 \frac{d < \varepsilon >}{dx_1} = \frac{7 < \varepsilon >^{3/2}}{3 \times 15^{1/2} \nu^{1/2}} \left(S + \frac{2G}{R_\lambda} \right) \qquad (14)$$

where $S \equiv< u_{1,1}^2 > / < u_{1,1}^2 >^{3/2}$ is the skewness of $u_{1,1}$ and $G \equiv< u_1^2 >< u_{1,11}^2 > / < u_{1,1}^2 >^2$ (Note: $u_{1,11} = \partial^2 u_1 / \partial x_1^2$). Eq. (14) was verified, to reasonable accuracy, by [11] using only single hot wire measurements at several locations downstream of the grid. As noted by [11], the terms on the right of (14) dominate this equation; the term on the left representing the small difference between the dissipation and production terms on the right side of that equation. A general transport equation for $<\chi>$ was first written by Corrsin [12], who compared it with the equation for $<\omega^2>\equiv<\omega_i\omega_i>$. In decaying grid turbulence, Corrsin's equation reduces to [13]

$$\frac{d\langle \chi \rangle}{dt} = 2\kappa \left\langle \theta_{,i} \theta_{,j} u_{i,j} \right\rangle - 2\kappa \left\langle \theta_{,j} \nabla^2 \theta_{,j} \right\rangle \qquad (15)$$

The two invariants on the right side of (15) represent the creation of $<\chi>$ through the stretching of the temperature field by the turbulent strain rate and the destruction of $<\chi>$ through molecular smoothing. For stationary turbulence and at sufficiently large Reynolds numbers, there is approximate equality between the terms on the right of either (13) or (15). Using isotropic forms of $<\theta_{,i}\theta_{,j}u_{i,j}>$ and $<\theta_{,j}\nabla^2\theta_{,j}>$ as given in [14], Eq. (15) can be simplified to

$$-U_1 \frac{d\langle \chi \rangle}{dx_1} = \frac{\langle \chi \rangle \langle \varepsilon \rangle^{1/2}}{\nu^{1/2}} \left[\left(\frac{5}{3} \right)^{1/2} S_T + \frac{10}{9} \frac{G_\theta}{Pe} \left(\frac{\Pr}{R} \right)^{1/2} \right] \qquad (16)$$

where $\Pr \equiv \nu / \kappa$ is the Prandtl number, $Pe \equiv u_1' \lambda_\theta / \kappa$ is the turbulent Péclet number, $\lambda_\theta \equiv \theta' / \theta_{,1}'$ is the Corrsin microscale and $R \equiv \theta'^2 < \varepsilon > /(< q^2 >< \chi >)$ is the energy-temperature dissipation timescale ratio. The parameters S_T and G_θ are defined as $S_T =< \theta_{,1}^2 u_{1,1} > / u_{1,1}^{'} < \theta_{,1}^2 >$ and $G_\theta =< \theta_{,11}^2 > \theta'^2 / < \theta_{,1}^2 >^2$ respectively. By using the decaying relations for $<\varepsilon>$ and $<\chi>$ (Eqs. 3 and 4), the transport equations for $<\varepsilon>$ (14) and $<\chi>$ (16) can be recast as (e.g. [14])

$$G = \frac{15}{7} \left(1 + \frac{1}{n} \right) - \frac{S R_\lambda}{2} \qquad (17)$$

$$\frac{G_\theta}{R} = \frac{9}{10} \left(\frac{m+1}{n} \right) - \frac{9}{10} S_T R_\lambda \qquad (18)$$

Note that Eq. (17) reduces to the expression given in [11] when n=1. Eqs. (17) and (18) can be interpreted as equations for G and G_θ. Alternatively, they can also be interpreted as equations for n and m; they would then represent a relatively stringent test of the measured values of G and G_θ.

In the present study, the values for S and S_T are about −0.45 and −0.4 respectively. The estimation of G and G_θ requires $< u_{1,11}^2 > \equiv \int_0^\infty k_1^4 \phi_{u_1}(k_1) dk$ and $< \theta_{,11}^2 > \equiv \int_0^\infty k_1^4 \phi_\theta(k_1) dk$ to be determined properly. To obtain adequate closure of the above integrands, the measured distributions of ϕ_{u_1} and ϕ_θ are first corrected for spatial resolution using the procedures outlined in [13] and then extrapolated beyond the low-pass filter cut-off frequency to allow adequate convergence of the above integrals. The method outlined in [15] was adopted for extrapolation; at sufficiently large k_1^*, the spectra ϕ_{u_1} and ϕ_θ has the form $k_1^{*-5/3} \exp(\alpha k_1^* + \beta)$ (where α and β are constants). A linear extrapolation can then be used on a $\log[k_1^{*5/3} \phi_{u_1}^*(k_1^*)]$ or $\log[k_1^{*5/3} \phi_\theta^*(k_1^*)]$ vs k_1^* plot. The values of $< u_{1,11}^2 >$ and $< \theta_{,11}^2 >$ can subsequently be obtained from the integrands $\int_0^\infty k_1^4 \phi_{u_1}(k_1) dk$ and $\int_0^\infty k_1^4 \phi_\theta(k_1) dk$. The resulting values of G and G_θ, as shown in Figures 5(a,b), are equal to about 12.1 and 14.3 respectively, and are approximately constant with respect to x_1. G and G_θ can also be obtained with (17) and (18). They are compared in Figures 5(a,b) with the directly measured values. The good agreement between the measured and calculated values of G and G_θ indicates that the present probe performs satisfactorily.

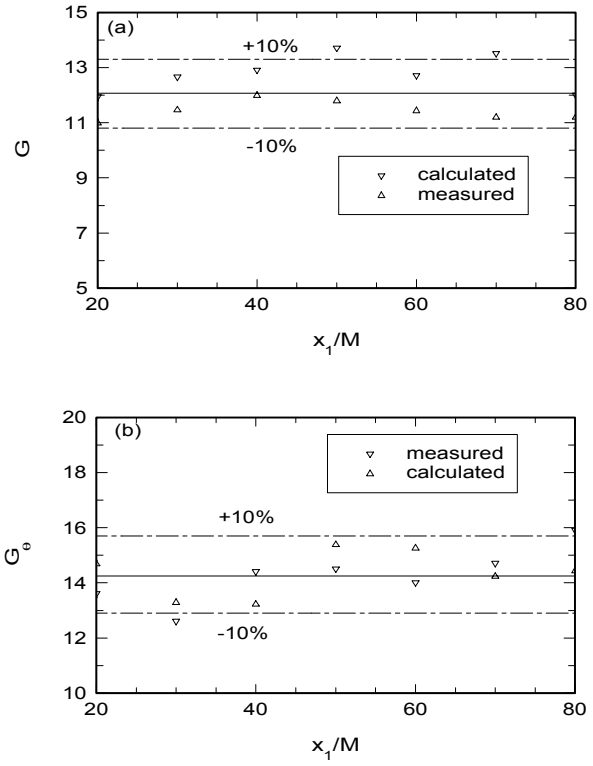

Figure 5. Comparison of (a): G and (b): G_θ between measurement and calculation. ∇: measurement; Δ: Calculation; — - —: range of ±10% of the averaged values (—) between measurement and calculation.

Conclusions

Instantaneous energy and temperature dissipation rates are measured simultaneously in decaying grid turbulence using a probe consisting of 4 X-wires (a total of 8 hot wires operated in constant temperature mode) and 2 pairs of parallel cold wires (operated in constant current mode). Extensive checks were made to test the performance of the probe. The directly measured values of the mean energy and temperature dissipation rates agree within ±10% with those obtained from the streamwise decay rates of the mean energy and the temperature variance. The probe also yields all three fluctuating vorticity components; their spectra are in close agreement with isotropic calculations, almost independently of the wavenumber; their variances are also consistent with isotropy [Eq. (12)]. Transport equations for the energy and temperature dissipation rates are closely satisfied by the data obtained from this probe. The measured instantaneous values ε and χ are expected to be good approximations to the true instantaneous dissipation rates.

Acknowledgement

RAA gratefully acknowledges the support of the Australian Research Council.

References

[1] Wallace, J. M. and Foss, J. F., The measurement of vorticity in turbulent flows, Ann. Rev. Fluid Mech., **27**, 1995, 467-514.

[2] Anselmet, F., Djeridi, H. and Fulachier, L., Joint statistics of a passive scalar and its dissipation in turbulent flows, *J. Fluid Mech*. **280**, 1994, 173-197.

[3] Stolovitzky, G., Kailasnath, P. and Sreenivasan, K. R., Refined similarity hypotheses for passive scalars mixed by turbulence, *J. Fluid Mech.,* **297**, 1995, 275-291.

[4] Antonia, R. A., Browne, L. W. B. and Chambers, A. J., On the spectrum of the transverse derivatives of the streamwise velocity in a turbulent flow, Phys. Fluids, **27**, 1984, 2628-2631.

[5] Zhu, Y. and Antonia, R. A., Spatial resolution of a 4-X-wire vorticity probe, *Meas. Sci. & Technol*., **7**, 1996, 1492--1497.

[6] Zhou, T., Antonia, R. A., Lasserre, J-J., Coantic, M. and Anselmet, F., Transverse velocity and temperature derivative measurements in grid turbulence, 14th Australian Fluid Mechanics Conference, Adelaide University, Adelaide, Australia, December, 2001.

[7] Antonia, R. A., Zhou, T. and Zhu, Y., Three-component vorticity measurements in a turbulent grid flow, *J. Fluid Mech*., **374**, 1998, 29-57.

[8] Van Atta, C. W., Local isotropy of the smallest scales of urbulent scalar and velocity fields, *Proc. Roy. Soc. Lond*., **A434**, 1991, 139-147.

[9] Antonia, R. A. and Mi, J. Corrections for velocity and temperature derivatives in turbulent flows, *Expts. in Fluids*, **14**, 1993, 203-208.

[10] von Kármán, T. The fundamentals of the statistical theory of turbulence, *J. Aero. Sci*., **4**, 1937, 131-138.

[11] Batchelor, G. K. and Townsend, A. A., Decay of vorticity in isotropic turbulence, *Proc. Roy. Soc. Lond*. **A190**, 1947, 534--550.

[12] Corrsin, S., Remarks on turbulent heat transfer: an account of some features of the phenomenon in fully turbulent regions, *Proc. Iowa Thermodynamics Symposium*, State University of Iowa, 1953, 5-30.

[13] Wyngaard, J. C., The effect of velocity sensitivity on temperature derivative statistics in isotropic turbulence*, J. Fluid Mech*., **48**, 1971, 763-769.

[14] Zhou, T., Antonia, R. A., Danaila, L. and Anselmet, F., Transport equations for the mean energy and temperature dissipation rates in grid turbulence*, Expts. in Fluids,* **28**, 1998, 143-151.

[15] Pearson, B. R., Experiments on small-scale turbulence, PhD thesis, The University of Newcastle, Australia, 1999.